Remarkable Dynamic NMR Spectra and Properties of a Sterically Congested *cis*-1,2-Diarylcyclobutane

David A. Ben-Efraim* and Rina Arad-Yellin*
Department of Organic Chemistry, The Weizmann Institute of Science, Rehovot 76100, Israel

Dimethyl 2,2'-dichloro-6,6'-dimethoxy-β-truxinate **2** displays in solution, by ^{1}H NMR spectroscopy, a mixture of two conformers: a *meso* conformer and a racemic conformer. The other possible *meso* conformer may be present in a small amount in solution. The NMR parameters of these conformers were extracted from their low-temperature static ^{1}H and ^{13}C spectra. The conformers interconvert mainly by a mechanism involving rotation of one aryl group at a time. Activation parameters of the same dynamic process were obtained by band-shape simulations from four different regions of the variable-temperature ^{1}H spectra. In one spectral region, rate constants in excess of 10^6 s^{-1} were recorded.

Dimethyl 2,2',6,6'-tetrachloro-β-truxinate [dimethyl 3β,4β-bis(2,6-dichlorophenyl)-1α,2α-cyclobutanedicarboxylate] **1** was shown by band-shape analysis of its dynamic ^{1}H and ^{13}C spectra to display restricted rotation of its aryl groups.[1] The origin of the phenomenon in this type of compound was also discussed.[1] Its close relative, dimethyl bis(2-chloro-6-methoxy)-β-truxinate [dimethyl 3β,4β-bis(2-chloro-6-methoxyphenyl)-1α,2α-cyclobutanedicarboxylate] **2**, is endowed with a uniqueness unparalleled in the annals of dynamic NMR spectroscopy.[2] It embraces four independent ^{1}H spectral regions which exhibit the same act of restricted rotation of the aryl groups, and in one region the dynamic process was measured and simulated by total band-shape analysis in steps of 10 K in a range spanned by 215 K, culminating in rate constants in excess of 10^6 s^{-1}. The significance of complex spectra, large temperature and chemical shift ranges, and a large number of data points for the computation of reliable activation parameters in dynamic NMR was stressed.[2f,3] Compound **2** is a case in point because its ^{1}H spectra possess these characteristics and the activation parameters can be computed and compared in four different regions. Most dynamic NMR studies were done at coalescence temperatures, or by band-shape analysis, but only at a few temperatures and in a single spectral region.[2] This paper concentrates on the static and dynamic NMR spectra of **2**, deferring discussion of the geometry of its conformers and their relation to NMR parameters, to another paper. As will be detailed for each region separately, it can be discerned at once from the low-temperature spectra that **2** exists in solution as a mixture of three conformers: a *meso* conformer, *meso*-**2A** (with averaged C_s symmetry), and two enantiomeric conformers, (+)-**2** and (−)-**2** (with C_1 symmetry) (Fig. 1). A second possible *meso* conformer *meso*-**2B** is invisible in the NMR spectrum but may be present in a small amount in solution. Whereas the two aryl groups of *meso*-**2A** possess the same NMR properties, those of (±)-**2** have different properties from each other. These differences are also reflected in the spectral properties of the other three regions, namely, the MeO, CO_2Me, and cyclobutane regions. The thermodynamic parameters ($\Delta H°$, $\Delta S°$) of the equilibrium between the two conformers were extracted from their population ratios at four temperatures (168 to 195 K) below the onset of the dynamic process by using the linear form of Boltzmann's distribution law. The same value of $\Delta H°$ was also obtained by integration of van 't Hoff's equation. For K = (+)-**2** [or (−)-**2**]/*meso*-**2A**, $\Delta H°$ = 1.09 ± 0.13 kJ mol^{-1} and $\Delta S°$ = 4.01 ± 0.75 mol^{-1} K^{-1}. This indicates that inversion of conformer stability occurs around 273 K. The entropy difference $\Delta S°$ due to enantiomer mixing in (±)-**2** should be at least equal to R ln 2 (5.77 J mol^{-1} K^{-1}), and its reduced value may be due to steric interference between the aryl groups of (±)-**2**.

Results

Aromatic Region.—The chemical shifts and coupling constants of the static spectrum at 184 K (Fig. 2) were extracted from a series of double-irradiation experiments (Table 1) and were verified by simulation and by comparison with the spectrum at the fast-exchange limit at room temperature: δ 6.404 (dd, 1-, 4-, 9-H), 6.756 (dd, 3-, 6-, 7-H) and 6.872 (t, 2-, 5-, 8-H). The corresponding average chemical shifts calculated from the static parameters and from the conformer populations at 184 K are δ 6.456, 6.795 and 6.952, whereas those computed from substituent additivity constants[4] are δ 6.71, 6.83 and 6.94. The correspondence is quite good, except for the proton *ortho* to the MeO group, because the substituent constants were not meant for heavily substituted benzene rings.[4]

Scheme 1 displays all the possible interconversions among the four possible conformers, albeit only three of them are visible in the ^{1}H NMR spectrum (and ^{13}C spectrum) at 184 K. Therefore, simulations could be carried out in all four regions of the ^{1}H spectrum only among these three conformers [*meso*-**2A**, (+)-**2** and (−)-**2**] for which chemical shifts and coupling constants are available (Table 1). In fact, when simulations were done with rotations of only one aryl group at a time, excellent fits with experimental spectra were obtained in the aromatic region (Fig. 2 and Table 2). Chemical shift differences within each aryl group showed poor dependence on temperature.

Methoxy Region.—The static spectrum at 184 K (Fig. 3) indicates that the two high-field singlets of equal areas should be assigned to the two MeO groups of (±)-**2** and the low-field singlet should be assigned to the methoxy groups of *meso*-**2** (Table 1). This is corroborated by NOE difference observations. Thus, irradiation of 1-, 2- and 3-Me enhances the intensities of 1-, 4- and 9-H, respectively. In addition, these NOE spectra revealed that irradiation of 1-Me of *meso*-**2A** showed no enhancement of cyclobutane hydrogens and thus its conformation is tentatively assumed to have its methoxy groups on the outside. By contrast, irradiation of 3-Me of (±)-**2** enhanced 17-H, whereas irradiation of 2-Me showed no enhancement, thus supporting the conformations given in Fig. 1. Simulations of the methoxy spectra were done, as in the case of the aromatic region, with rotation of one aryl group at a time (Scheme 1,

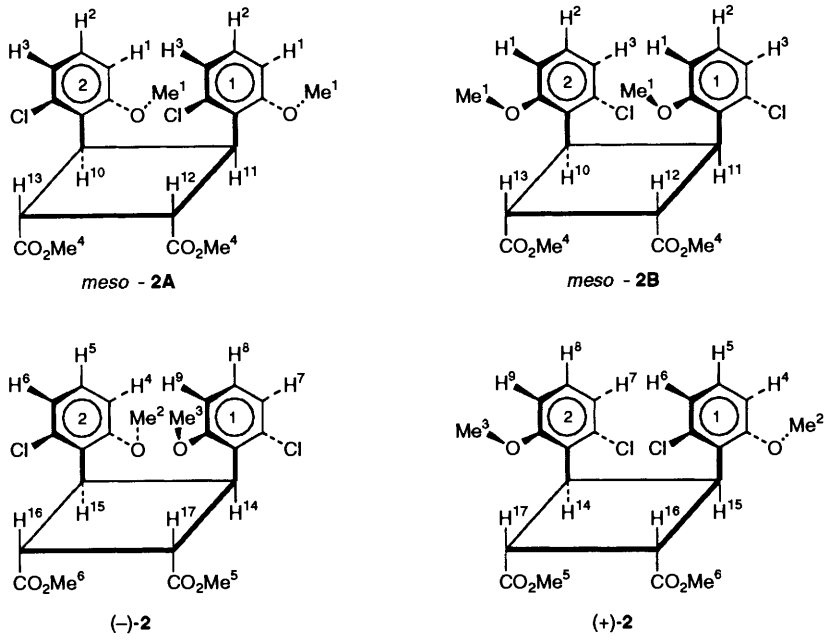

Fig. 1 Conformations of **2**. The (+) and (−) assignments in (±)-**2** are arbitrary.

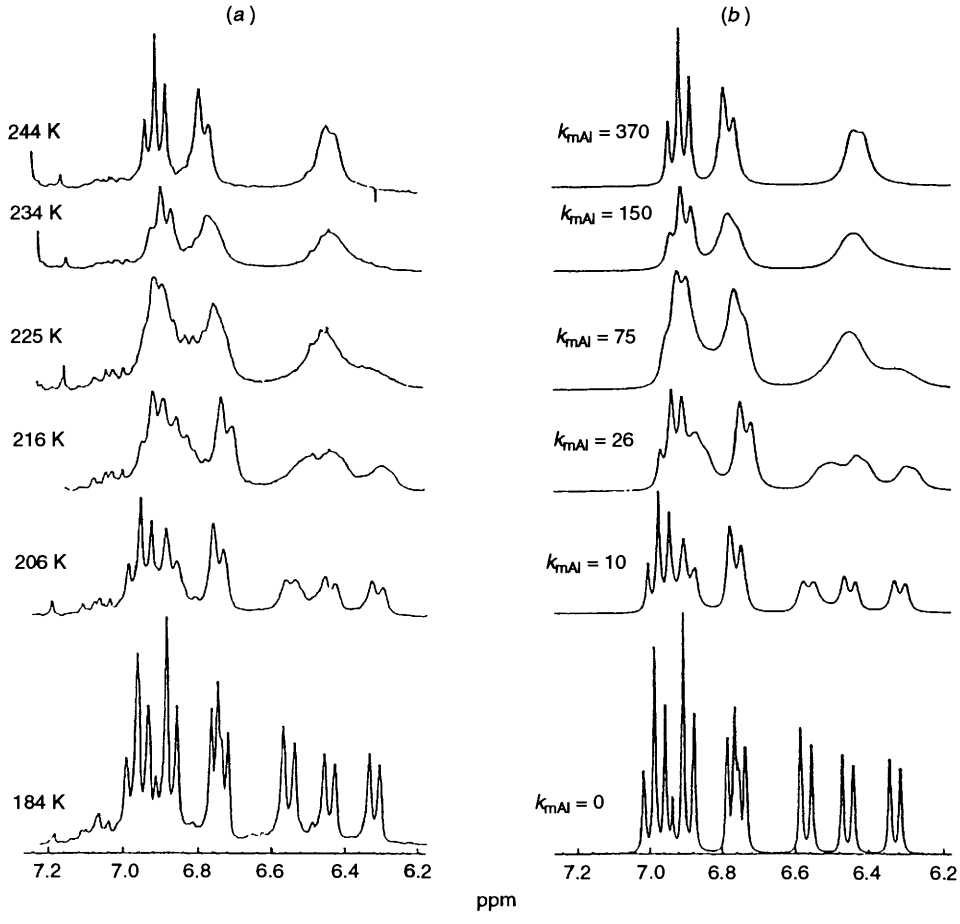

Fig. 2 Experimental (*a*) and simulated (*b*) static ^1H spectrum (184 K) and representative dynamic spectra of the aromatic region of **2** in CS_2–$CDCl_3$ (3:1)

Table 2 and Fig. 3). In these simulations rotations about the C_{sp^2}–O bond was ignored, as rotational barriers about this bond are less than *ca.* 17 kJ mol^{-1} and thus are too fast on the NMR timescale.[5]

Carbomethoxy Region.—The CO_2Me groups do not participate directly in the aryl rotations. They do rotate on the C–CO_2Me bonds with rates which are too fast on the NMR timescale. Thus the three closely spaced and partially overlapping singlets in the static spectrum at 184 K (Fig. 3) arise from the effect of the slow rotations of the three aryl groups upon the averaged conformations of the fast rotating CO_2Me groups (Table 1). Again as in the aromatic and MeO regions, simulations of the variable-temperature spectra were done with

Table 1 ^{1}H Chemical shifts (ppm) and coupling constants (Hz) of **2A**

Aromatic region, CS_2–$CDCl_3$ (3:1), 184 K												
meso-**2A**	H1	6.571	H2	6.986	H3	6.752	$J_{1,2}$	8.335	$J_{1,3}$	1.000	$J_{2,3}$	7.901
(±)-**2**	H4	6.330	H5	6.903	H6	6.772	$J_{4,5}$	8.023	$J_{4,6}$	1.000	$J_{5,6}$	8.292
	H7	6.895	H8	6.980	H9	6.458	$J_{7,8}$	7.842	$J_{7,9}$	0.799	$J_{8,9}$	8.344
Cyclobutane region, CS_2–$CDCl_3$ (3:1), 184 K												
meso-**2A**	H10, H11	4.795	H12, H13	4.444			$J_{10,11}$	11.330	$J_{10,12}$	−1.000		
							$J_{10,13}$	8.000	$J_{11,12}$	8.000		
							$J_{11,13}$	−1.000	$J_{12,13}$	11.340		
(±)-**2**	H14	4.699	H15	4.892			$J_{14,15}$	11.158	$J_{14,16}$	−1.000		
	H16	3.547	H17	5.345			$J_{14,17}$	4.840	$J_{15,16}$	10.890		
							$J_{15,17}$	−1.000	$J_{16,17}$	11.024		
Cyclobutane region (dynamic spectrum) [$^2H_6$]DMSO, 313 K												
meso-**2A**[a]	H10, H11	4.722	H12, H13	4.521	same coupling constants as in CS_2–$CDCl_3$ at 184 K							
(±)-**2**[a]	H14	4.757	H15	4.968	same coupling constants as in CS_2–$CDCl_3$ at 184 K							
	H16	3.547	H17	5.326								
Methoxy region, CS_2–$CDCl_3$ (3:1), 184 K												
meso-**2A**	Me1	3.606										
(±)-**2**	Me2	3.438										
	Me3	3.532										
Carbomethoxy region, $CFCl_3$–$CDCl_3$ (1.5:1), 184 K												
meso-**2A**	Me4	3.834										
(±)-**2**	Me5	3.813										
	Me6	3.806										

[a] Parameters used in spectral simulation.

Table 2 Rate constants $k_{mAl} = k_{mAd}$ (s^{-1}) of the dynamic process of **2** (part 1)

T/K	Aromatic region[a]	Methoxy region[a]	T/K	Carbomethoxy region[b]
195	2.5 ± 0.5	3 ± 1	198	1.5 ± 0.5
206	10 ± 1	10 ± 2	201	2 ± 0.5
216	26 ± 2	29 ± 2	206	3.5 ± 0.5
225	75 ± 5	75 ± 15	209	4 ± 0.5
234	150 ± 10		212	5.0 ± 0.75
244	370 ± 50		216	7 ± 1
253	800 ± 100			
262	1450 ± 200			

[a] In CS_2–$CDCl_3$ (3:1). [b] In $CFCl_3$–$CDCl_3$ (1.5:1).

rotations of one aryl group at a time (Scheme 1, Table 2 and Fig. 3). Interchange of populations in the simulations indicated the correct chemical shift assignments of the three carbomethoxy groups.

Cyclobutane Region.—The static spectrum of this region at 184 K (Fig. 4) supports more than any of the other regions, the assignment of the conformations of *meso*-**2A** and (±)-**2**. The two mirror-image bands are at once assigned to the AA'BB' spin system of *meso*-**2A** (Scheme 1). Four multiplets should be displayed by (±)-**2**, but only three are observed. A series of double resonance experiments elucidated the spin connectivities and showed that the fourth multiplet of (±)-**2** is hidden between the tails of 1- and 3-Me (Table 1). Table 1 also shows that the averages of the chemical shifts of the pairs 14-, 15-H and of 16-, 17-H of (±)-**2** are equal to the chemical shifts of 10-, 11-H and 12-, 13-H of *meso*-**2**, respectively, thus establishing the relationship between the protons of the interconverting conformers. This relationship between the protons of the two conformers is supported by saturation transfer difference experiments, done under NOE difference spectroscopy conditions.[6] Thus, even at 184 K, where the spectrum is assumed to be static, irradiation of the following protons yields negative bands of the protons given in parenthesis: 10-, 11-H (14-, 15-H); 12-, 13-H (17-H); 16-H (hidden multiplet) (12-, 13-H) and 17-H (12-, 13-H). The low-and high-field bands of *meso*-**2A** were assigned to 10-, 11-H and 12-, 13-H, respectively, on the following grounds: the methine protons of isopropylbenzene[7a] and methyl isobutyrate[7a] resonate at δ 2.89 and 2.48 ($\Delta\delta$ 0.41 ppm), respectively, and those of *cis*-1,2-diphenylcyclobutane,[7b] and of the monomethyl ester of *cis*-cyclobutane-1,2-dicarboxylic acid[7c] resonate at δ 3.79–4.12 and 3.3–3.6 ($\Delta\delta$ *ca.* 0.5 ppm), respectively. Thus methines bonded to aryl groups are shifted to low field relative to methines bonded to carboxylate groups.

As in the case of the CO_2Me region, the cyclobutane ring is not directly involved in the rotations of the aryl rings, but its dynamic behaviour in the NMR experiment is directly influenced by them (Scheme 1). Inversion of a puckered cyclobutane ring is too fast on the NMR timescale to be detected, because the barrier to interconversion is less than 8 kJ mol^{-1} and therefore it was ignored in the dynamic NMR

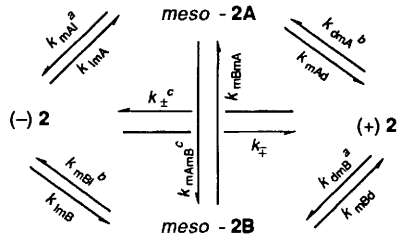

[a] Aryl 1 rotation. [b] Aryl 2 rotation. [c] Concerted aryl 1 and aryl 2 rotations.

$k_{mAl} = k_{mAd}$ $k_{mBl} = k_{mBd}$ $k_{lmA} = k_{dmA}$ $k_{lmB} = k_{dmB}$ $k_{\pm} = k_{\mp}$

Region	*meso*-**2A** or −**2B**	(−)-**2**	(+)-**2**	Averaged spectrum
Aromatic	ABC	DEF	GHI	ABC
Methoxy	A	B	C	A
Carbomethoxy	A	B	C	A
Cyclobutane	AA'BB'	CDEF	DCFE	AA'BB'

Scheme 1

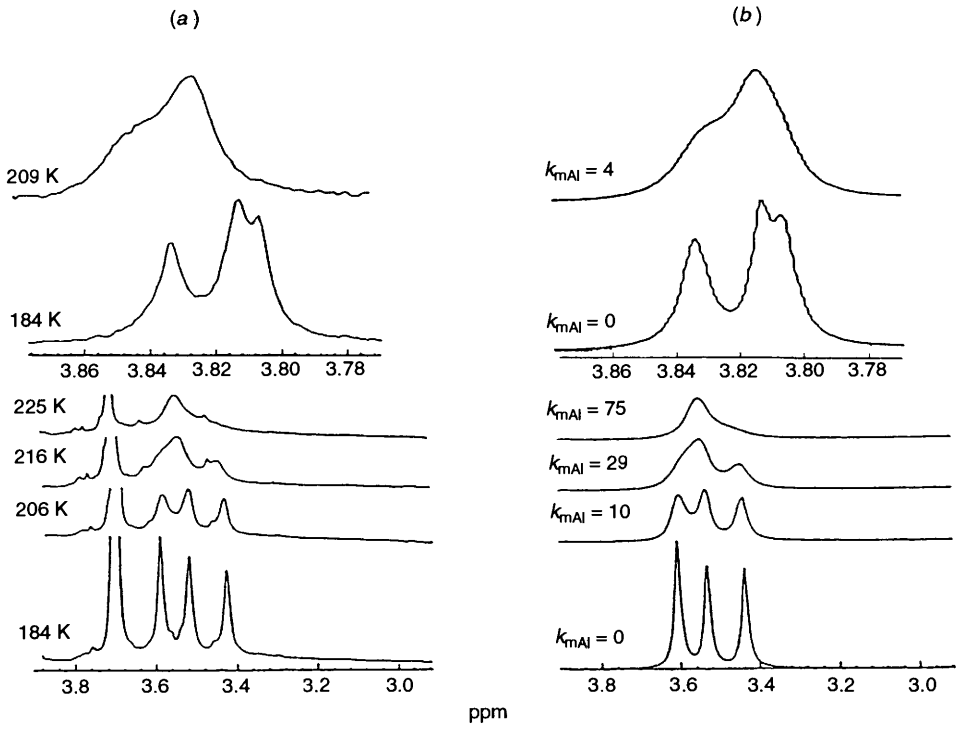

Fig. 3 Experimental (*a*) and simulated (*b*) static ^{1}H spectrum (184 K) and representative dynamic spectra of the methoxy region of **2** in CS_2–$CDCl_3$ (3 : 1) (four lower spectra), and static ^{1}H spectrum (184 K) and a representative dynamic spectrum of the carbomethoxy region of **2** in $CFCl_3$–$CDCl_3$ (1.5 : 1)

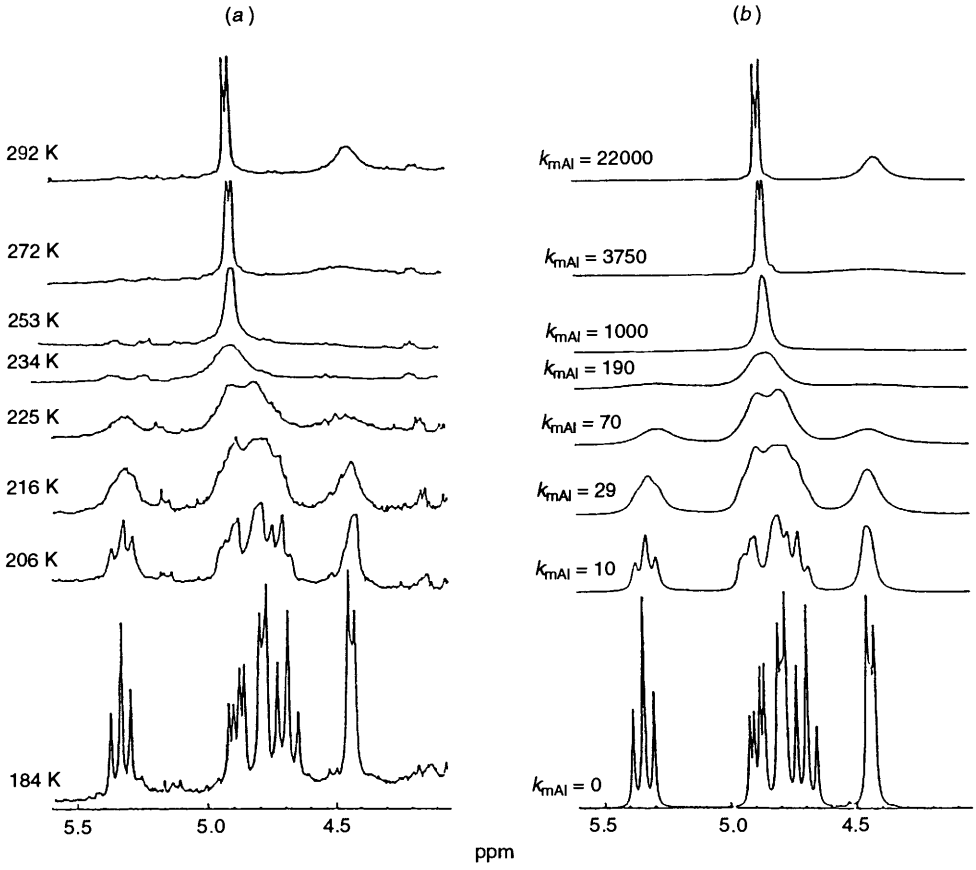

Fig. 4 Experimental (*a*) and simulated (*b*) static ^{1}H spectrum (184 K) and representative dynamic spectra of the cyclobutane region of **2** in CS_2–$CDCl_3$ (3 : 1). The high-field multiplet 16-H, hidden under 1- and 3-Me, is not shown.

simulations.[8] The chemical shift range of 16-, 17-H in (±)-**2** is very large (1.798 ppm), but that of 14-, 15-H is small (0.193 ppm) (Figs. 4 and 5). This is why the latter methines are already averaged at room temperature, whereas the evolution of the former to finally yield a simple AA'BB' spectrum demands a temperature rise from 184 to 400 K. Variable-temperature spectra were recorded in CS_2–$CDCl_3$ (195–336 K) and in [$^2H_6$]DMSO (315–399 K). Simulations of these spectra were

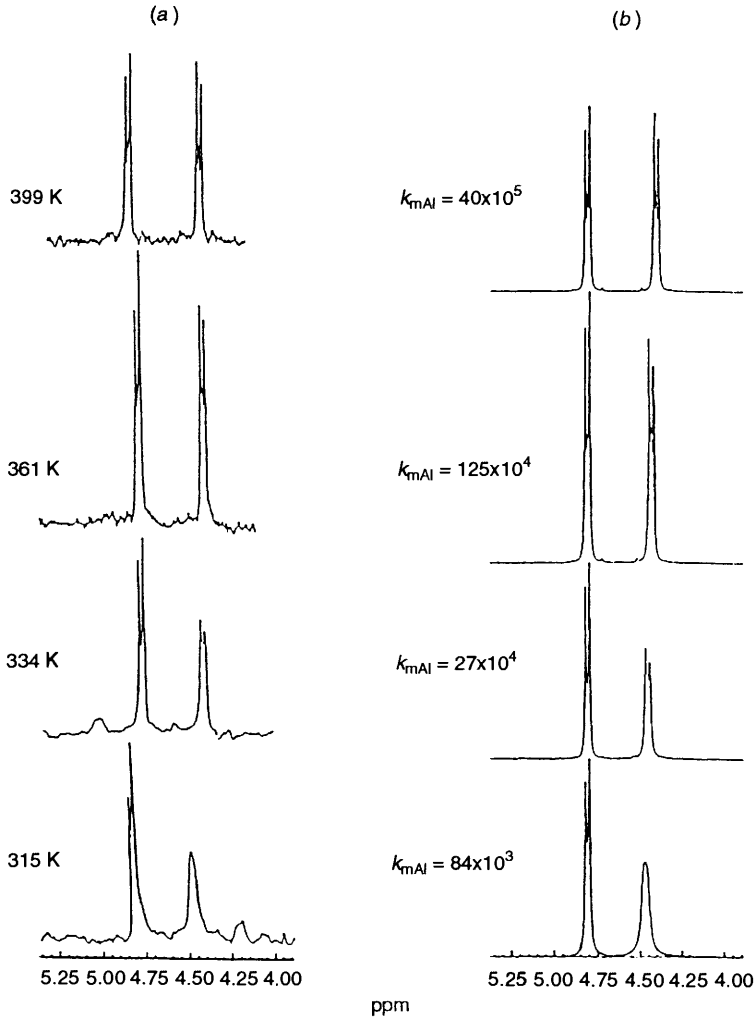

Fig. 5 Experimental (*a*) and simulated (*b*) representative dynamic spectra of the cyclobutane region of **2** in [$^2H_6$]DMSO. The high-field region of the hidden 16-H is not shown.

Table 3 Rate constants (s^{-1}) of the dynamic process of **2** in the cyclobutane region (part 2)

T/K	$k_{mAl} = k_{mAd}$ [a]	T/K	$k_{mAl} = k_{mAd}$ [b]
195	3	315	84 × 10^3
206	10	324	155 × 10^3
216	29	334	27 × 10^4
225	70	343	45 × 10^4
234	190	352	80 × 10^4
244	370	361	125 × 10^4
253	1 000	369	19 × 10^5
262	2 400	377	30 × 10^5
272	3 750	387	40 × 10^5
281	11 000	399	50 × 10^5
292	22 × 10^3		
298	35 × 10^3		
307	68 × 10^3		
317	120 × 10^3		
326	165 × 10^3		
336	255 × 10^3		

[a] In CS_2–$CDCl_3$ (3:1). [b] In [$^2H_6$]DMSO.

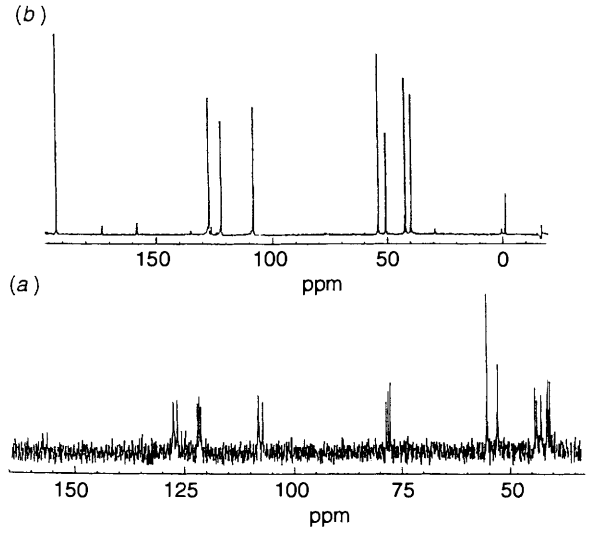

Fig. 6 ^{13}C Spectra of **2** at 184 K (*a*) in CS_2–$CDCl_3$ (3:1) and at room temperature (*b*) in CS_2–$CDCl_3$ (5:1)

done with rotation of one aryl group at a time (Figs. 4 and 5 and Table 3).

^{13}C NMR Spectra.—Comparison of the broad-band decoupled spectra of **2** at room temperature and at 199 K, confirms the conclusions reached on the basis of the ^1H NMR spectra, that only two conformers are observed by ^{13}C NMR in CS_2–$CDCl_3$ solution (Figs. 1 and 6). In the static spectrum at 199 K the *meso* and racemic conformers call for six peaks in the cyclobutane region (two *meso* and four racemic peaks) and three peaks for each carbon atom of the aromatic rings (one *meso* and two racemic peaks), and in fact all these peaks are observed (Table 4).[9] By contrast, the MeO peak is not split and remains sharp at low temperature. The methyl of the CO_2Me group, however, displays two very close peaks of unequal

Table 4 ^{13}C Chemical shifts (ppm) and coupling constants (Hz) of **2**

	Room temp.[a]			199 k[b]		
	δ	Calcd. δ[c]	Multiplicity and coupling constants[d]	δ		
Cyclobutane	40.72		dd, ^1J 138.7, ^3J 7.2	40.09	40.56	40.77
	43.10		dd, ^1J 142.7, ^3J 6.6	42.18	43.13	43.63
CO_2Me	51.32		q, ^1J 145.5	52.46	52.65	
*Me*O	54.67		q, ^1J 143.3	55.05		
*C*H(*o*-MeO)	107.86	111.9	dd, ^1J 157.7, ^3J 7.6	107.70	108.63	108.81
*C*H(*o*-Cl)	121.35	120.9	dd, ^1J 167.2, ^3J 8.1	121.95	122.32	122.69
C(*o*-MeO)	125.10	134.7		125.47	125.73	126.45
*C*H(*m*-MeO)	126.55	128.1	d, ^1J 162.0	127.29	128.03	128.30
C-Cl	133.83	133.6		135.48	135.77	136.24
C-MeO	156.98	159.1		157.53	158.44	158.66
CO_2Me	171.80					

[a] In CS_2–$CDCl_3$ (3:1). [b] In CS_2–$CDCl_3$ (5:1). [c] Calculated from substituent additivity constants.[9] The substituent constant of the isopropyl group was used for the cyclobutyl group. [d] Obtained from gated decoupling.

Table 5 Activation parameters of **2** and their standard deviations

Region	N[a]	$\Delta\delta$/Hz	T/K	r[b]	$\Delta H^{\ddagger}$/ kJ mol^{-1}	$\Delta S^{\ddagger}$/ J mol^{-1} K^{-1}	$\Delta G^{\ddagger}$(298.2 K)/ kJ mol^{-1}
Aromatic[c]	8	177.12	195–262	−0.9993	38.37 ± 0.59	−36.11 ± 2.51	49.12 ± 0.17
Methoxy[c]	4	45.36	195–225	−0.9991	37.49 ± 1.13	−39.71 ± 5.27	49.33 ± 0.46
Cyclobutane[c]	16	485.46	195–336	−0.9982	43.35 ± 0.71	−12.72 ± 2.68	47.15 ± 0.17
Cyclobutane[d]	10	480.33	315–399	−0.9962	50.12 ± 1.55	9.04 ± 4.29	47.41 ± 0.25
Carbomethoxy[e]	6	7.56	198–216	−0.9915	27.11 ± 1.76	−99.83 ± 8.49	56.86 ± 0.75

[a] Number of data points. [b] Correlation coefficient [$1/T$, ln (k/T)]. [c] In CS_2–$CDCl_3$ (3:1). [d] In [$^2H_6$]DMSO. [e] In $CFCl_3$–$CDCl_3$ (1.5:1).

intensities. Decoupled variable-temperature spectra, recorded at 225 and 240 K showed that the fast-exchange limit was almost attained at the higher temperature. The inability to distinguish between the *meso* and racemic peaks in the cyclobutane and aromatic regions made simulation of the spectra a hopeless task.

Discussion

Compound **2** presents a rare opportunity to extract and compare activation parameters of the same dynamic process from four different regions of the ^1H NMR spectrum by means of a total band-shape analysis, a case which is not abundant in the literature. In such a comparison the role of errors cannot be ignored. Many authors discussed the errors of the activation parameters extracted from a least-squares computation by means of the Eyring equation.[2a,3,10] The enthalpy of activation, and in particular $\Delta S^{\ddagger}$, are very sensitive to errors in rate constants, especially in the low- and high-field temperature extremes of the dynamic range.[11] The main culprit in this connection is the insensitivity of the rate constants, or for that matter, the insensitivity of the effective T_2s to large variations in temperature at the above extremes. This difficulty may be overcome by the use of complex spin systems which give rise to differential effects at the above temperature extremes.[1,1,3] In fact the spin systems of the aromatic and cyclobutane regions of **2** display strongly coupled second-order complex spectra below the onset of exchange. The spin systems also span large chemical shift ranges and large temperature intervals, and together with a substantially large number of exchange spectra contribute to obtaining reliable activation parameters. The activation parameters (Table 5) extracted from the different regions were quite close (so far as values in the same solvent mixture were compared), if in addition to statistical errors, other errors, such as temperature instabilities, dependence of linewidth on viscosity and variations in chemical shifts and populations are taken into account. Still, interconversion can be envisaged to take place also *via* the invisible, relatively unstable *meso*-**2B** conformer as shown in Scheme 1. If this invisible conformer had energy higher by 12 kJ mol^{-1}, its population would be only 0.02% at 180 K and thus be undetectable by NMR. Also concurrent contributions from concerted rotations of two aryl groups at a time in addition to rotation of one aryl group at a time cannot unequivocally be excluded at higher temperatures in the cyclobutane region as simulation with good fits were obtained, but such a process may be highly improbable. Cases which deal with rotational exchange between a *meso* conformer and the enantiomers of a racemic conformer, as in our case, were reported. Oki *et al.*[12] investigated in depth such a case in 9-benzyltriptycenes, the spectra of which were simulated with two independent rates of rotation, and it was concluded that the uncertainties in the values of the rate constants could not be erased. In the case of (*E*)-1,2-diethyl-1,2-di-*tert*-butylethylene it was shown that the main dynamic process involved the rotation of only one ethyl group at a time, between a cisoid conformer and one enantiomer of a transoid conformer, but that 30% of the process may have involved concerted rotation of two ethyl groups between the enantiomers of the transoid conformer.[13] In still another case the rotations of the 3- and 4-isopropyl groups in 3,4-diisopropylthiazole-2(3*H*)-thiones were shown to be non-synchronous.[14]

A compound close to **2** is *cis*-1-mesityl-2-phenylcyclopentane.[15] The restricted rotation of its mesityl groups has a $\Delta G^{\ddagger}$ of *ca.* 46 kJ mol^{-1} at 229 K, whereas in its torsionally rigid analogues *cis*-1-phenyl-2-mesitylacenaphthene and 5-bromo-*cis*-1-phenyl-2-(2,4,6-trimethyl-3-bromophenyl)acenaphthene, the $\Delta G^{\ddagger}$s of the restricted rotation of the substituted phenyl groups are larger than 105 kJ mol^{-1} at 473 and 349 K, respectively. It is tempting to compare the activation parameters of **2** with those of **1**.[1] It is found that $\Delta H^{\ddagger}$ of **2** is smaller than $\Delta H^{\ddagger}$ of **1** by *ca.* 8 kJ mol^{-1}. It was argued that in **1** the two aryl groups are perpendicular to each other and that the major contribution to $\Delta G^{\ddagger}$ had its origin in the interaction of the two chlorine atoms from the two adjacent aryl groups, and

only to a lesser extent from the interaction between the aryl groups themselves.[1] The C(aryl)–Cl bond length is *ca.* 1.75 Å, whereas the bond lengths of C(aryl)–O and O–Me are *ca.* 1.37 and 1.42 Å, respectively, the angle C(aryl)–O–Me being *ca.* 120°. Also the van der Waals radius of oxygen (1.40 Å) is smaller than that of chlorine (1.80 Å), and Eliel[16] pointed out that racemization of biphenyls *via* planar transition states is much faster when they are substituted in the *ortho* position with methoxy groups rather than with chloro groups. Methoxy groups bonded to aromatic rings are generally *syn* to an *ortho* hydrogen when the other *ortho* position is blocked. Thus as was shown in the MeO region, NOE irradiation of each methoxy group enhanced the intensity of the corresponding *ortho* hydrogen. It was also reported that in the crystal lattice of *ortho*-monosubstituted methoxybenzenes, MeO is *syn* to the *ortho* hydrogen.[17] In the ground states of **1** and of the conformers of **2** the interactions between the substituents on the two aryl groups are insignificant. In the transition states with only one aryl group rotating, however, the situation is different. In **1** the C(aryl)–Cl bond is rigid and points in the transition state in the direction of the other aryl group and its C(aryl)–Cl bond. By contrast, in the transition state of **2**, the rotating aryl group has the choice to turn its MeO group, rather than its chloro group, towards the other aryl group. The Me–O bond can then avoid an interaction with that aryl group because it does not point in its direction. As a consequence of all the above considerations, the steric interference in the transition state of **2** is smaller than that in **1**, and as a result $\Delta H^{\ddagger}$ of *meso*-**2** is smaller than that of **1**. If in fact the approach of the MeO group of one aryl group towards the other aryl group in the transition state of **2** predominates, this leads to the notion that a one-ring flip is in operation in **2**, in which one aryl group oscillates clockwise and anticlockwise between *meso*-**2** and the enantiomers of (±)-**2**, with its MeO end always pointing in the direction of the other aryl group.[18] Also the MeO substituent of the rotating aryl group in the one-ring flip mechanism {*meso*-**2**⇌(+)[(−)]-**2**} proposed here, enjoys more freedom of motion in the ground state than in the transition state, resulting in a negative contribution of $\Delta S^{\ddagger}$. Thus, in **2**, in addition to the larger restricted motion of the aryl group itself in the transition state, there is the above loss of freedom of motion of the MeO group. This is missing in the transition state of **1** and therefore *meso*-**2A** has a more negative $\Delta S^{\ddagger}$ than **1** (by *ca.* 21 J mol^{-1} K^{-1}).

Experimental

NMR Measurements.—NMR spectra with 16 K data points were recorded on a Bruker WH-270 NMR spectrometer in FT mode, operating at 270 MHz (^1H) and at 67.889 MHz (^{13}C). Sample solutions were degassed by three freeze–thaw cycles and sealed under reduced pressure in 5 mm (^1H) and 10 mm (^{13}C) od precision NMR tubes. The concentrations of **2** were 0.02 mol dm^{-3} (^1H) and 0.16 mol dm^{-3} (^{13}C) in CS_2–$CDCl_3$ (^1H, 3:1 and ^{13}C, 3:1 and 5:1), $CFCl_3$–$CDCl_3$ (1.5:1), and [$^2H_6$]-DMSO. Me_4Si served as internal standard at the lower temperatures and the [$^2H_5$]DMSO signal at 2.49 ppm served the same purpose at the high temperatures. The chemical shift differences in the spectra of MeOH and ethylene glycol were used for the determination of low and high temperatures of the ^1H NMR spectra, respectively.[19a] The chemical shift differences in the spectrum of MeI–Me_4Si was similarly used to determine the temperatures of the ^{13}C NMR spectra.[19b] These measurements were taken before and after recording each spectrum and the average chemical shift difference was used to obtain the temperature. The thermometer liquid was kept 5 min in the probe before reading the chemical shift difference. The thermometer liquids were not calibrated with a thermocouple.

Computations.—Static and dynamic spectra were simulated with computer program DNMR5,[20] using 1024 data points and were visually fitted to the experimental spectra. Dimensions of several variables in this program were expanded to accommodate the dynamic four-spin cyclobutane system, and the program was modified to allow for large rate constants observed in this region. For the simulations and visual fittings the parameters were handled as follows: chemical shift differences in the aromatic region showed scatter with respect to temperature and the chemical shifts were moved to fit peaks of experimental spectra. Chemical shifts of (±)-**2** in the cyclobutane region were kept practically constant with only minor adjustments, whereas the chemical shift difference of *meso*-**2** was linearly dependent on temperature and was adjusted accordingly. The coupling constants of the static spectra were used in the variable-temperature simulations. Long-range benzylic coupling and coupling between MeO and the aryl group were ignored, although they were reported as being a source of systematic errors in the calculation of activation parameters from ^1H NMR total band-shape analysis.[21] Population ratios of the two conformers were obtained below the onset of the dynamic process at 168, 173, 184 and 195 K, by weighing areas in three of the four spectral regions of the CS_2–$CDCl_3$ spectra. These values were somewhat erratic but it was possible to extract thermodynamic parameters ($\Delta H°$, $\Delta S°$) from them. The temperature-dependent population ratios were used in the spectral simulations and were obtained from the above calculated thermodynamic parameters. These population ratios were also used in the simulations in $CFCl_3$–$CDCl_3$ (CO_2Me region) and [$^2H_6$]DMSO (cyclobutane region). Effective T_2 values were estimated according to Sandstrom's formula:[22] in CS_2–$CDCl_3$ and $CFCl_3$–$CDCl_3$ the linewidth of a sharp peak of **2** at 184 K was used together with the linewidths of the $CHCl_3$ signal from the static and dynamic spectra, but T_2 for solutions in [$^2H_6$]DMSO was obtained from sharp signals of MeO and CO_2Me. The T_2 values were moderately varied in the simulations to fit the experimental linewidths. The errors in rate constants were determined by simulation with smaller and larger rate constants until changes in intensities and line shapes started to appear. Half the interval between the extreme rate constants was taken as the error, but in the cyclobutane region a fixed 20% error in the rate constants was used in the calculation of the activation parameters. Activation parameters ($\Delta H^{\ddagger}$, $\Delta S^{\ddagger}$) and their errors were computed, using the Eyring equation, and linear as well as non-linear least-squares programs from the literature,[23] all yielding the same results. These equations weigh errors in both temperatures and rate constants. A fixed-temperature error of 1 K was used in all calculations. The errors in free energies of activation were calculated according to Binsch *et al.*[10f]

(E)-2-*Chloro*-6-*methoxycinnamic Acid.*—(*Z*)-2-Chloro-6-methoxycinnamic acid[24] was sublimed in high vacuum (< 1 mmHg/230 °C) to yield the (*E*)-acid (90%), m.p. 195–196 °C. High vacuum and short heating times are imperative, otherwise decarboxylation of the (*E*)-acid occurs; δ_H[90 MHz; $(CD_3)_2CO$] 3.95 (3 H, s, OMe), 6.88 (1 H, d, *J* 16, H_α), 8.09 (1 H, d, *J* 16, H_β), 7.05–7.45 (3 H, m, ArH), 8.36 (1 H, br s, CO_2H).

Dimethyl 2,2′-*Dichloro*-6,6′-*dimethoxy*-β-*truxinate* **2**.—Samples of (*E*)-2-chloro-6-methoxycinnamic acid were spread between window-glass plates and were irradiated with Westinghouse sunlamp for 15 days at 5 °C. TLC ($MeCO_2Et$–C_6H_6–Me_2CO, 5:4:1) showed, besides unreacted monomer, a less mobile spot of **2**. Conversion was *ca.* 80% as calculated from relative areas of MeO peaks in ^1H NMR). The mixture of crude acids in MeOH solution, containing a few drops of $SOCl_2$, was refluxed for 2 h to yield a mixture of their methyl esters. The

esters were separated by preparative TLC and were identified as (*E*)-methyl 2-chloro-6-methoxycinnamate[24] and **2**. The latter was recrystallized from Pr^{i}OH, affording white crystals, m.p. 124–125 °C (Found: C, 58.0; H, 5.0; Cl, 15.6. $C_{22}H_{22}Cl_2O_6$ requires C, 58.29; H, 4.89; Cl, 15.64); λ_{max}(MeOH)/nm 278 (ε/dm^3 mol^{-1} cm^{-1} 3900) and 285 (3900); ν_{max}(KBr)/cm^{-1} 2945w, 1739s, 1576m, 1459s, 1261s, 1045s and 760m; *m*/*z* 452.065 (M^+, $C_{22}H_{22}O_6{}^{35}Cl_2$, 2.2%) and 226.040 (9.6, symmetric cleavage to monomer, $M^+/2$, $C_{11}H_{11}O_3{}^{35}Cl$).

References

1 D. A. Ben-Efraim and R. Arad-Yellin, *Tetrahedron*, 1988, **44**, 6175.
2 (*a*) G. Binsch, *Top. Stereochem.*, 1968, **3**, 97; (*b*) J. Sandstrom, *Dynamic NMR Spectroscopy*, Academic Press, London, 1982; (*c*) M. Oki, *Applications of Dynamic NMR Spectroscopy to Organic Chemistry*, VCH, Deerfield Beach, FL, 1985; (*d*) K. Umemoto and K. Ouchi, *Proc. Indian Acad. Sci., Chem. Sci.*, 1985, **94**, 1; (*e*) U. Berg and J. Sandstrom, *Adv. Phys. Org. Chem.*, 1989, **25**, 1; (*f*) K. G. Orrell, V. Sik and D. Stephenson, *Prog. Nucl. Magn. Reson. Spectrosc.*, 1990, **22**, 141.
3 G. Binsch and H. Kessler, *Angew. Chem., Int. Ed. Engl.*, 1980, **19**, 411.
4 L. M. Jackman and S. Sternhell, *Applications of Nuclear Magnetic Resonance Spectroscopy in Organic Chemistry*, Pergamon Press, Oxford, 1969, pp. 201–204.
5 (*a*) T. Schaefer and R. Sebastian, *Can. J. Chem.*, 1989, **67**, 1148; (*b*) D. C. Spellmeyer, P. D. J. Grootenhuis, M. D. Miller, L. F. Kuyper and P. A. Kollman, *J. Phys. Chem.*, 1990, **94**, 4483.
6 J. K. M. Sanders and B. K. Hunter, *Modern NMR Spectroscopy*, Oxford University Press, Oxford, 1988, pp. 218–219 and 224–234.
7 (*a*) Ref. 4, p. 164; (*b*) R. M. Dodson and A. G. Zielske, *J. Org. Chem.*, 1967, **32**, 28; (*c*) C. C. Shroff, W. S. Stewart, S. J. Uhm and J. W. Wheeler, *J. Org. Chem.*, 1971, **36**, 3356.
8 R. M. Moriarty, *Top. Stereochem.*, 1974, **8**, 271.
9 D. F. Ewing, *Org. Magn. Reson.*, 1979, **12**, 499.
10 (*a*) A. Allerhand, F.-M. Chen and H. S. Gutowsky, *J. Chem. Phys.*, 1965, **42**, 3040; (*b*) J. A. Ladd and H. W. Wardale, in *Internal Rotation in Molecules*, ed. W. J. Orville-Thomas, Wiley, London, 1974, pp. 131–135; (*c*) V. M. Gittins, E. Wyn-Jones and R. F. M. White, in ref. 10(*b*), p. 454; (*d*) G. Binsch, in *Dynamic Nuclear Magnetic Resonance Spectroscopy*, eds. L. M. Jackman and F. A. Cotton, Academic Press, New York, 1975, pp. 75–78; (*e*) U. Berg, S. Karlsson and J. Sandstrom, *Org. Magn. Reson.*, 1977, **10**, 117; (*f*) D. Hofner, H. Tamir and G. Binsch, *Org. Magn. Reson.*, 1978, **11**, 172; (*g*) M. H. Chang and D. A. Dougherty, *J. Am. Chem. Soc.*, 1983, **105**, 4102; (*h*) M. H. Chang, B. B. Masek and D. A. Dougherty, *J. Am. Chem. Soc.*, 1985, **107**, 1124.
11 D. Hofner, S. A. Lesko and G. Binsch, *Org. Magn. Reson.*, 1978, **11**, 179.
12 M. Oki, M. Kono, H. Kihara and N. Nakamura, *Bull. Chem. Soc. Jpn.*, 1979, **52**, 1686.
13 D. Lenoir, D. Malwitz and B. Meyer, *Tetrahedron Lett.*, 1984, **25**, 2965.
14 (*a*) A. Liden, C. Roussel, M. Chanon, J. Metzger and J. Sandstrom, *Tetrahedron Lett.*, 1974, 3629; (*b*) C. Roussel, A. Liden, M. Chanon, J. Metzger and J. Sandstrom, *J. Am. Chem. Soc.*, 1976, **98**, 2847.
15 A. R. Miller and D. Y. Curtin, *J. Am. Chem. Soc.*, 1976, **98**, 1860.
16 E. L. Eliel, *Stereochemistry of Carbon Compounds*, McGraw-Hill, New York, 1962, pp. 159–160.
17 W. Hummel, K. Huml and H.-B. Burgi, *Helv. Chim. Acta*, 1988, **71**, 1291.
18 (*a*) R. Blom, *Acta Chem. Scand., Ser. A*, 1988, **42**, 445; (*b*) S. E. Biali and Z. Rappoport, *J. Org. Chem.*, 1986, **51**, 2245; (*c*) J. E. Anderson, P. A. Kirsch and J. S. Lomas, *J. Chem. Soc., Chem. Commun.*, 1988, 1065; (*d*) J. E. Anderson, R. W. Franck and W. L. Mandella, *J. Am. Chem. Soc.*, 1972, **94**, 4608; (*e*) R. L. Clough and J. D. Roberts, *J. Am. Chem. Soc.*, 1976, **98**, 1018.
19 M. L. Martin, G. J. Martin and J.-J. Delpuech, *Practical NMR Spectroscopy*, Heyden, London, 1980: (*a*) pp. 445–446; (*b*) pp. 337–338.
20 D. S. Stephenson and G. Binsch, *QCPE*, 1978, **10**, 365.
21 T. Drakenberg and R. E. Carter, *Org. Magn. Reson.*, 1975, **7**, 307.
22 A. Liden and J. Sandstrom, *Tetrahedron*, 1971, **27**, 2893.
23 (*a*) J. A. Irvin and T. I. Quickenden, *J. Chem. Educ.*, 1983, **60**, 711; (*b*) M. Lybanon, *Am. J. Phys.*, 1984, **52**, 22.
24 R. Arad-Yellin, B. S. Green and K. A. Muszkat, *J. Org. Chem.*, 1983, **48**, 2578.

Paper 3/06170A
Received 15*th October* 1993
Accepted 11*th January* 1994